

# Refining Efficiency for Future CTMP and TMP systems

## Co-optimizing Fundamental Wood Material Knowledge with a Soft Sensor Control Approach

Anders Karlström\*, Per Engstrand\*\*, \*Chalmers University of Technology, Göteborg, Sweden, \*\*Mid Sweden University, Sundsvall, Sweden

---

**KEYWORDS:** Modeling, CTMP, energy efficiency, pulp consistency, fiber residence time, fiber-to-bar interaction, temperature profile, motor load distribution

**SUMMARY:** Internal variables in (C)TMP-refining processes (e.g. temperature, consistency, fiber residence time, backward flowing steam and forces acting upon the chips and pulp) are defined as physical states obtained in different parts of the refining zones. In short, they differ from the traditional external variables (e.g. dilution water feed rate, load and gap distance) which are not available as distributed variables from refining zone measurements.

The internal variables are the backbone of physical models and such models can be used for on-line implementation of soft sensors and advanced process control. Of special interest are the temperature and consistency profiles together with fiber residence time, which are the internal variables in focus of (in) this study. Moreover, they are directly linked to pulp and handsheet property development.

To illustrate the capability to use a modeling strategy, two examples are given; one where it is shown how to reach a 40% reduction in specific energy in a CD82-refiner using a new control strategy without violating the pulp properties studied and one example where the consistency can be controlled individually in two parallel Twin refining zones. Hence, the article comprises both temperature and consistency control to reach optimal process conditions.

We believe that increased fundamental understanding of the role of the spatially dependent viscosity in refining in general will be a key factor to find ways to further improve energy efficiency of refining.

---

### ADDRESSES OF THE AUTHORS:

Anders Karlström ([anderska@chalmers.se](mailto:anderska@chalmers.se)), Sweden

Per Engstrand ([per.engstrand@miun.se](mailto:per.engstrand@miun.se)), Sweden

**Corresponding author: Anders Karlström**

---

Several approaches have been proposed over the years to describe how to find proper operating points for good enough pulp quality and minimized energy demand (consumption) in refining processes. Most papers dealing with refiner optimization and control confine themselves to discussing the topic either with the perspective of an individual refiner or an individual TMP production line, see Hill et al. (1979), Johansson et al. (1980), Dahlqvist and Ferrari (1981), Oksum (1983), Honkasalo et al. (1989), Hill et al. (1993), Berg (2005), Eriksson (2005) and Eriksson (2009).

During the late 1980s, Miles and May (1990, 1991) derived a theoretical model of the pulp flow behavior in the refining zone of a high consistency (HC) refiner. The theory became widely used and increased the understanding of refining to some extent.

Miles and May (1990, 1991) introduced the concept of refining intensity, which was defined as the ratio between the specific energy (i.e. the relation between motor load and the assumed production rate) and the number of fiber-to-bar interactions (or the fiber residence time), see Kure (1999). Miles and May (1990, 1991) used uni-directional refiner segments, where the idea was to define a scalar that describes the bar-to-fiber impact estimated for the entire refining zone, see further Strand et al. (1993) and Murton et al. (2002). Furthermore, suggestions to describe the connection between control variables on refining zone conditions and pulp properties were published by Stationwala et al (1991).

Sabourin et al. (2001) claimed that the model derived by Miles and May (1990, 1991) is not suitable for practical use since it has too many unknown parameters and variables. One example was the friction coefficients introduced to describe the interaction between the refining segment surface and the pulp. Isaksson et al. (1997) had shown this earlier and concluded that the proposed friction coefficients are far from the values estimated in full-scale refiners and that the coefficients varied dramatically for different refining conditions.

Svensson et al. was first to build an equipment with which sliding friction between steel and wood at high temperatures in saturated steam could be measured (2006). In connection to this, the influence of chemical conditions related to CTMP process conditions have been investigated by Logenius et al (2014) as well. Fundamental aspects of strain rates of wood at elevated temperatures relevant for TMP and CTMP refining conditions have only been studied by means of the Encapsulated Split Hopkinson Pressure bar equipment (ESHP) at FSCN Mid Sweden University first described by Holmgren et al. (2008). Several studies utilizing the ESHP have since then been performed in cooperation especially with VTT and Tampere University (TUT) (Moilainen et al 2016, Salmi et al 2012, Björkqvist et al 2012). In short the results from these experiments tells us that within the temperature and pulp consistency range prevalent in a typical high consistency primary stage and secondary stage refiners influence of temperature level even with a change of only a few degrees will have a large impact on the compressibility of the fibers. The interpretation of friction is extremely difficult as it is affected by softening, which is influenced by the temperature level that changes over the gap. Furthermore, it is shown that the chemical environment prevalent in the gap depend on in the chemical environment with regard to pH and metal ion composition in which the wood chips have been pretreated. The choice of type of dilution water will also have a large impact on swelling and softening behavior of the wood fibers and fiber walls see Engstrand et al (1991)

and Fjellström et al. 2012 and 2013). In this paper, we have chosen to use the concept of viscous dissipation instead of introducing friction as a common physical variable. The reason for this is, besides for what is mentioned above, that it from a fluid dynamic perspective is interesting and probably more relevant to discuss the defibration/fibrillation inside the refining zone in terms of spatial shear force and dynamic/kinematic viscosity vectors. We believe that it is very important to consider the quite large change in conditions along the gap of refiners when creating models describing the refining process.

Some key background information related to this work was created in the “Filling the Gap project” performed in cooperation between Chalmers Industriteknik and FSCN at Mid Sweden University with strong support from the pulp & paper, supplier and consultant companies; Norske Skog, Holmen, SCA, Stora Enso, Dametric, Metso/Valmet och Poyry, 2009-13 (Engstrand et al 2011 and 2014).

To this time, process models, based on first principals, had been used off-line for analysis, see Karlström and Eriksson (2014a, b,c,d) and Karlström and Hill (2014a,b and 2015a,b). One reason why the implementation of such models on-line has taken such a long time is that the model complexity sometimes itself introduces barriers due to limited computer capacity. Another reason is that these models produce a huge amount of data that must be handled in real-time. However, now the time has come where the computer capacity is not a problem anymore, see Karlström and Hill (2016a, b, c).

This paper presents how to use soft sensors, i.e. models on-line. The models comprise a complete refiner including systems descriptions for inlet mixing zones, refining zones and outlet mixing zones and it is easy to extent to include serially linked refiners as well as reject refiners. The model copes with real-time process changes and is assumed to be the backbone in future control concepts for CD- and Twin refiners. The focus is on control issues where the interplay between internal variables (e.g. temperature and consistency) and external variables (e.g. dilution water feed rate, specific energy and plate clearance) are vital.

The distinction between internal and external variables as indicated above was introduced by Karlström and Isaksson (2009) and further developed in Karlström et al. (2015 and 2016a,b). It was shown that using internal variables instead of external variables to find proper piece-wise linear models, estimating pulp and handsheet properties, gave a better opportunity to handle inherent non-linearities in the process. These results were to some extent not expected, as the major efforts to find models of pulp and handsheet properties had thus so far been based on external variables as independent variables, see Strand (1996), Strand and Grace (2014) and Lehtonen et al. (2014).

Data from full-scale production lines (CTMP: CD82-refiner and TMP: Twin-refiners) are here used to illustrate the need to implement physical models on-line for process optimization and control.

## Material and methods

Several attempts to model refining processes have been made after Miles and Mays’ (1990, 1991) contributions. To understand the process better spatial refining zone temperature measurements were introduced early by Atack et al (1975) and several follow-up studies were performed since then to improve the understanding of steam peak and steam flow distribution. Berg (2005), Karlström et al. (2005), Eriksson (2009) and Karlström et al. (2008) introduced spatial temperature measurements inside the refining zone to span the material and energy balances. This led to the possibility to span the distributed work as well, Karlström (2013).

The flow pattern in the refining zone is set by three physical states (chips/fibers ( $m_1$ ), water ( $m_2$ ) and vapor ( $m_3$ )) that must be considered simultaneously. The steam generated in the refining zone is commonly assumed to be saturated i.e. the pressure is a function of the temperature and vice versa, regardless of which type of high-consistency refiner is studied.

From a modeling perspective, it is important that the physical properties are available at different radial positions and scales as these variables are dependent on e.g. type of refining segments and actual process conditions. It is also important that the model can handle the energy input (motor load) as a distributed work in the refining zone from a macro-scale perspective.

Karlström and Eriksson (2014a) also started using gap distance in order to estimate the distributed viscosity profile in a CD-82 refiner, see Fig. 1. This expansion formed the “extended entropy model,” which was a set of material and energy balances for one refining zone. The concept was developed even further and is now used as an important tool for soft sensors in Twin refiners.

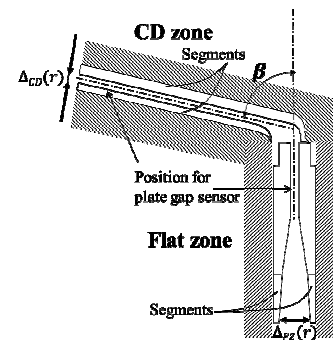


Fig. 1: A schematic drawing of the refining zones in a CD refiner. The vertical flat zone (FZ) is directly linked to the conical zone (CD) via an expanding point.

The reason why the model refers to the entropy instead of the enthalpy is that the entropy generation

$$dS(r) = \frac{dE(r)}{T(r)}$$

is introduced as an important variable to distinguish between thermodynamic work given by the change in enthalpy and defibration/fibrillation work. Thus,  $dE$  refers to the energy dissipated and  $T$  is the absolute temperature.

In former model assumptions (May and Miles (1990)) a pure enthalpy balance was considered,  $dH=dE$ , where  $dH$  is the enthalpy generation, which did not consider the irreversible work related to the fiber development, i.e. the entropy generation,  $dS$ , in an infinitesimal control volume is assumed to be given by the expression for the viscous dissipation,  $\delta$  (Bird et al. 1960).

$$dS(r) = \frac{\delta(r)}{T(r)} \Delta(r) 2\pi r dr \quad (1)$$

where

$$\delta(r) = \mu \left( \frac{r\omega}{\Delta(r)} \right)^2 = \frac{w_R(r)}{\Delta(r)}$$

Thus it will be important to measure both the temperature profile  $T(r)$  and the plate gap profiles  $\Delta(r)$  in the refining zone, together with the entire motor load  $w_R$ , when deriving the dynamic viscosity  $\mu(r)$ .

Measuring the temperature profile is important for many reasons. One important reason is related to the question of where to find the position of the temperature maximum. As the steam evacuates both forwards (towards the periphery of the segments) and backwards (towards the inlet), the position can be seen as a stagnation point, which implies a zero pressure gradient,  $\partial P/\partial r$ . This is an important information for all types of refiners including Twin refiners as well as CD-refiners.

**Example I:** CD-refiners have two temperature profiles, see Fig. 2, i.e. it can be seen as two serially linked refiners.

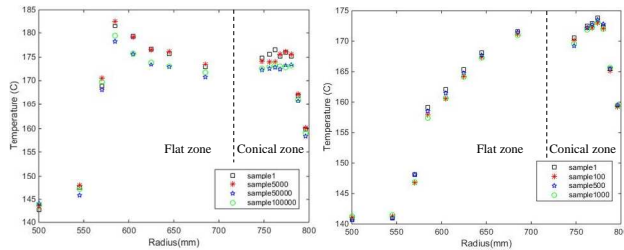


Fig. 2: Temperature profiles at two different test trials and the same type of refining segments. Plots spread over 1000 samples (seconds) in a CD82 refiner.

The stagnation points depend on the design of refining segments used; Sometimes two stagnation points are obtained as in case of a CD refiner, see Fig. 2.

Although the stagnation points in CD refiners are sometimes overlooked, it turns out that they are vital when deriving both backward and forward flowing steam. It was recently shown especially important to stabilize the position of the maximum temperature when using “low energy segments” (typically a more feeding segment compared to traditional) to avoid large steam fluctuations in the refining zone and the feeding position in the inlet. This might be considered obvious but temperature profiles are often not available for more advanced refiner control, which makes it difficult to foresee fiber pad fluctuations by only studying the specific energy variations, see Fig. 3.

When modeling refining zone conditions, the position for the stagnation point also becomes important as the steam balance affects a number of internal variables, e.g. the consistency profile.

The extended entropy model is to some extent complex and only briefly described in Appendix. The model was verified by Karlström et al. (2015, 2016a,b) for a number of test series in a full-scale CD82 refiner. This gave the possibility to even further analyze different process conditions related to other internal variables such as distributed defibration work, forces obtained when fibers interacted with the bars and grooves in the refining zone.

As the modeling of the refiners is an essential step towards a better understanding of the process, the reader is referred to Karlström et al. (2008) and Karlström and Eriksson (2014a,b,c,d) where the extended entropy model is described in details.

To expand the model to cover most of the equipment surrounding a refiner, we introduce different blocks as illustrated in Fig. 4.

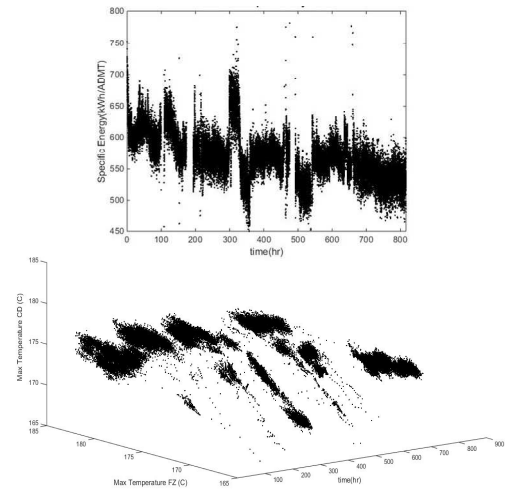


Fig. 3: Upper figure: Specific energy vs. time. Lower figure: Temperature in FZ and CD vs. time.

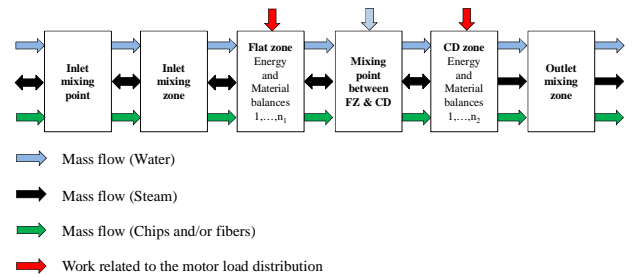


Fig. 4: Schematic description of the material and energy balances spanning the CD refiner.

In Fig. 4, the inlet mixing point is the position where wood chips meet dilution water added to the inlet zone while the inlet mixing zone corresponds to the zone close to the flat zone, where the inlet pressure of possible added steam meets the chips and water. The flat zone (FZ) energy and material balances  $I, \dots, n_1$  comprises  $n_1$  sensors where detailed information about the process can be derived. The mixing point between flat zone and CD

zone: illustrates the position where the dilution water is added to the CD zone. This is a central variable as it is vital for the distributed work and for the consistency estimations. The CD zone energy and material balances  $1, \dots, n_2$  comprises  $n_2$  sensors and is in many aspects similar to the corresponding FZ-block. The Outlet mixing zone describes the mass flows out from the CD zone. Most often this zone is associated with a flash calculation, as the temperature and pressure are normally lower in this position compared with inside the CD zone.

It is important to mention that the entropy model is a physical non-linear model which still can be used in on-line applications at sampling rates down to one second if the DCS can provide enough computer capacity.

When it comes to control concepts for refiners the strategy differs from one mill to another. Refining is well known to be a complex process with many disturbances and interactions. In some cases, refiners have an internal interconnection, in terms of piping from the outlet to the inlet, which makes control even more challenging. However, many similarities exist between different types of refiners, especially when having access to internal variables like temperature profile, consistency and fiber residence time.

**Example II:** Twin refiners have two parallel refining zones (FS and DS), see Fig. 5.

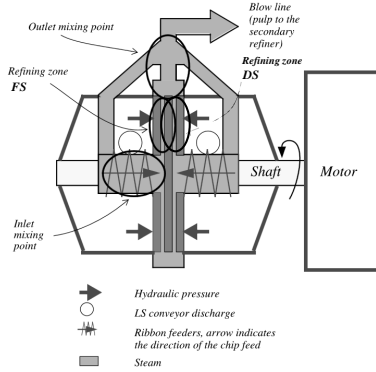


Fig. 5: Schematic description of a twin-disc refiner. The defibration/fibrillation is performed in two refining zones divided by a rotor. The refining zones are normally called the Front Side (FS) and the Drive Side (DS). The casing (outlet) is interconnected with the inlet mixing point in the primary refiner to even out the steam pressure and stabilize the feeding system.

The motor load ( $W$ ), hydraulic pressure (or plate gaps) ( $g$ ), mixing of chips or pulp ( $m_i$ ), steam ( $m_s$ ) and water added<sup>1</sup> ( $D$ ) are introduced as prime inputs in Twin refiner models. The models based on an enthalpy approach combined with an entropy approach similar to the one described for a CD-refiner. The direction of the steam flow is dependent on actual process conditions in a hypothetical mixing point. The direction of steam flow is primarily set by an iterative routine where the entropy models, illustrated by the second block i.e. the lower figure in Fig. 6, are involved as well.

<sup>1</sup> The total water added includes sealing water and dilution water. Internal water flows are denoted as  $m_2$ .

When modeling Twin refiners, the complexity increases as the inlet and outlet are interconnected in the primary refiner as illustrated in Fig. 5 while the secondary refiner is interconnected with the primary stage cyclones. All this makes it difficult to foresee the steam direction on beforehand without modeling the system. It is worth mentioning that the process design can differ significantly and is site specific.

In total, the material and energy balances comprises three mixing models for the primary refiner and two for the secondary refiner. The extended entropy model for each refiner is built on seven sub-models each. For details, the reader is referred to Appendix.

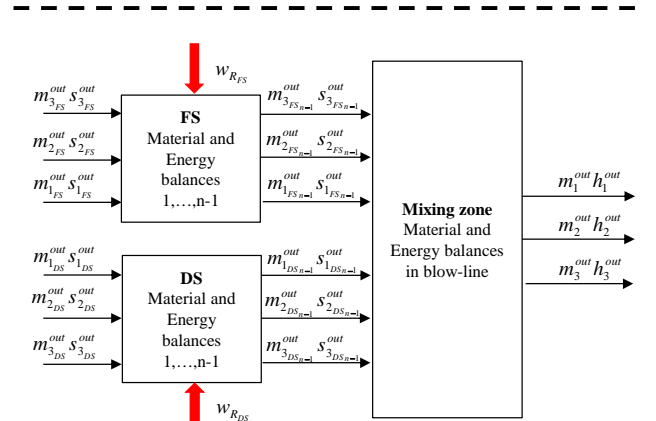
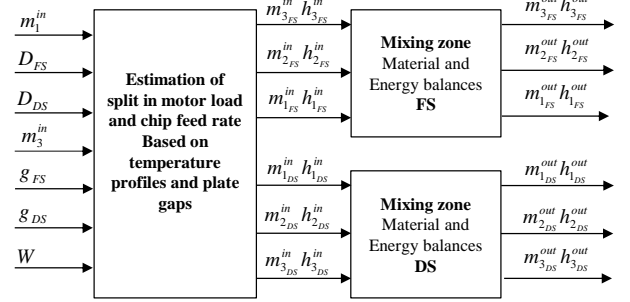


Fig. 6: Schematic illustration of the material and energy balances for each Twin-refiner. The mass flows are represented by  $m$ . The variables  $h$  and  $s$  represent the enthalpy and entropy, respectively.

As, the plate gaps are measured in each refining zone together with the temperature profiles it is possible to approach the problem with an uneven feed distribution to the refining zones.

In Fig. 7, the two temperature profiles on FS and DS in a primary and a secondary refiner are shown and it is obvious that the process conditions in the refining zones differ quite much also in a dynamic perspective and this knowledge is important to handle with care when modelling the internal variables such as consistency.

No further details about modeling issues are given in this paper and the reader is referred to Karlström and Hill (2015a,b,c,d) for details. Instead, the focus will be on how to use the models for analysis and optimization.



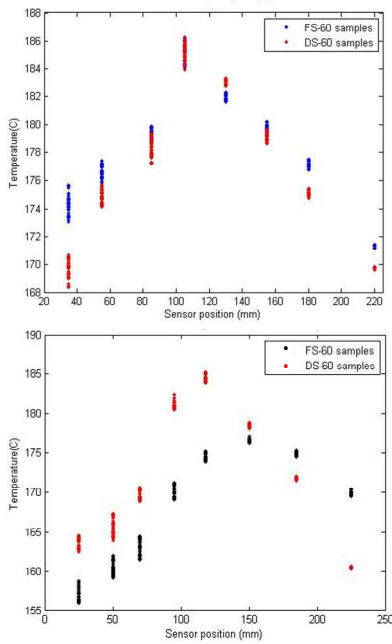


Fig. 7: Upper figure: Temperature profiles in a primary Twin refiner. Lower figure: Temperature profiles in a secondary Twin refiner. 60 samples correspond to one-hour operation.

## Results and discussion

There is no doubt that the temperature measurements can be seen as internal variables measured inside the refining zone. Such measurements together with traditional process variables, such as dilution water flows, plate gaps and specific energy are vital in terms of spanning the material and energy balances. The traditional process variables are consequently called external variables as they are measured outside the refiner or, like the plate gaps, can be classified as not typical physical phenomena<sup>2</sup>.

It is easy to understand that using a model that describes the major physical phenomena in a refining zone provides a possibility to predict several other internal variables such as:

- Fiber residence time (which is actually possible to define spatially dependent on segment pattern etc.)
- Consistency profile (which can be used as vector or divided into scalars in terms of e.g. blow-line consistency)
- Forces on bars (see Karlström and Eriksson (2014a,b) for details)
- Defibration work and thermodynamic work (which is important for the entire steam balance)
- Back-flowing steam (which can be used in future algorithms to predict incoming chip moisture)
- Pulp, water velocity and steam velocity (vital when analyzing e.g. feeding problems at different production levels)

<sup>2</sup> In this context, the specific energy is also classified as an external variable even though the motor load, which is the integral of all work distribution in the refining zone, can be seen as an internal variable.

As seen above, the extended entropy model is not a dynamic model based on partial differential equations. This was motivated by Karlström et al. (2008) as a consequence of the extremely fast dynamics in the refining zone (as mean value ranging from 0.5 to 1 second) together with the slower actuator dynamics for plate gap changes and the overall dominant dynamics in the inlet and outlet piping. All this limits the possibilities to control the refiner fast enough to cope with the instant refining zone dynamics, see the further discussion in Karlström and Hill (2014a,b, 2015a,b). However, the combination of fast and slow dynamics also opens the possibility for a robust on-line implementation of the equations described above. It is valuable to stress this.

**Example I:** From a control engineering perspective we start with a simplified description with two serially linked systems (i.e. two serially linked refining zones – FZ and CD) where all disturbances have been excluded, see Fig. 1.

The process input vector  $u=[S,D,P]$ , consists of the elements plate gap or hydraulic pressure for closing the refining zone ( $S$ ) dilution water feed rate ( $D$ ) and production, i.e. wood chip feed rate ( $P$ ). The production is the same in both refining zones while the plate gap and dilution water added are individual for each zone and therefore divided according to  $[S_{FZ}, D_{FZ}]$  and  $[S_{CD}, D_{CD}]$ , respectively.

If the internal variables are not available for control, which is the most common situation in the pulp and paper industry, the system description using the specific energy  $y_E$  (i.e. the ratio of the motor load to the production rate<sup>3</sup>) and the estimated consistency in the blow-line  $y_C$  become

$$y = \begin{bmatrix} y_E \\ y_C \end{bmatrix} = Gu = \begin{bmatrix} g_{11} & g_{12} & g_{13} & g_{14} & g_{15} \\ g_{21} & g_{22} & g_{23} & g_{24} & g_{25} \end{bmatrix} \begin{bmatrix} S_{FZ} \\ D_{FZ} \\ S_{CD} \\ D_{CD} \\ P \end{bmatrix} \quad (2)$$

The drawback with this process description is that the specific energy is impossible to split into the defibration/fibrillation work in FZ and CD, respectively. Moreover, specific energy is non-linear dependent on changes in the input vector which is cumbersome when introducing more advanced MPC control concepts. By using internal variables instead, a more sophisticated control concept can be formulated.

The internal variable sets  $[T_{maxFZ}, C_{FZ}]$  and  $[T_{maxCD}, C_{CD}]$ , comprising the maximum temperatures and the consistencies, give together with the pulp quality  $Q$  the simplest form of the output vector  $y$  to be controlled. Moreover, as shown by Karlström and Hill (2014a,b,c,d), the system complexity can be reduced when measuring the temperature profile due to natural decoupling phenomena, see Eq.3.

<sup>3</sup> The motor load is normally seen as an output while the production rate, i.e. the chip feed rate to the refiner line is an input. Therefore, from a control engineering perspective the specific energy control concept is questionable.

$$y = \begin{bmatrix} T_{\max_{FZ}} \\ C_{FZ} \\ T_{\max_{CD}} \\ C_{CD} \\ Q \end{bmatrix} = Gu = \begin{bmatrix} g_{11} & & & & g_{15} \\ & g_{22} & & & g_{25} \\ & & g_{33} & & g_{35} \\ & g_{42} & g_{44} & g_{45} & \\ g_{51} & g_{52} & g_{53} & g_{54} & g_{55} \end{bmatrix} \begin{bmatrix} S_{FZ} \\ D_{FZ} \\ S_{CD} \\ D_{CD} \\ P \end{bmatrix} \quad (3)$$

where  $G$  is the transfer function matrix describing the process dynamics. Hence in total we have a  $5 \times 5$ -system<sup>4</sup> to handle. The benefit, however, is that the system can be described by a sparse matrix as seen in Eq. 3.

Normally, the aim is to keep the production as stable as possible. Any disturbance in production is captured by the temperature profile measurements and other internal variables like consistencies, see Karlström and Hill (2014a,b,c,d). As a result, the complexity can be reduced even further. Consider a cascade controller where the pulp quality  $Q$ , is controlled by using a simplified MPC-concept based on measurement data obtained from devices positioned after the latency chest or estimation routines based on the information from the extended entropy model. We have already concluded that it will be necessary to cope with the element  $g_{42} \neq 0$ , i.e. the consistency in the flat zone, as it affects the consistency in the CD-zone. This results in a system description that is quite reasonable to handle by all system engineers.

$$y = \begin{bmatrix} T_{\max_{FZ}} \\ C_{FZ} \\ T_{\max_{CD}} \\ C_{CD} \end{bmatrix} = Gu = \begin{bmatrix} g_{11} & & & \\ & g_{22} & & \\ & & g_{33} & \\ & g_{42} & g_{44} & \end{bmatrix} \begin{bmatrix} S_{FZ} \\ D_{FZ} \\ S_{CD} \\ D_{CD} \end{bmatrix} \quad (4)$$

As the consistency out from the flat and conical zones will be possible to estimate, see Appendix, the extended entropy model can be seen as a soft sensor.

To illustrate how to use internal variables for process analysis and control, the test according to Fig. 8 was performed.

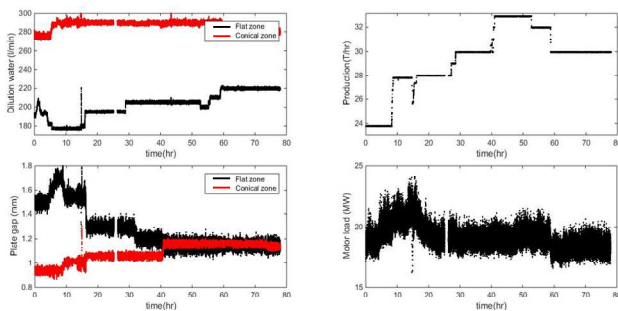


Fig. 8: Step changes performed in the external variables of dilution water (upper left), production (upper right) and plate gap (middle left); response in motor load including time for each test point (middle right).

Initially, it was difficult to increase the production, and manipulation of the plate gap and dilution water to the CD zone were too risky in a pulp quality perspective.

As the main target was to increase the production rate, the operators had to open the plate gap in the conical zone at the same time as the plate gap was reduced in the

flat zone. In other words, a better refiner controllability was provided. The operators requested more information about the process conditions in the flat zone before changing the operating point; to overcome that problem, the extended entropy model was used before and after each step change in the plate gap, dilution water feed rate and production.

As seen in Fig. 9, the temperature maximum position can fluctuate dramatically depending on different process conditions. At the high production level achieved after 40h when CD gap was opened up, the FZ temperature increase at constant load, probably both due to increased chip flow and decreased FZ gap. In Fig. 10 the dynamic viscosity is shown to be lower at the highest flow-rate when the temperature is at its highest level where wood fibers are known to be more easily fibrillated. The temperature profile shown, is quite flat which means that the position of the zero pressure gradient,  $\partial P/\partial r=0$ , can vary and thereby cause fluctuating backward and forward flowing steams. This is not an optimal situation and calls for further attention in coming control concepts where it is wise to introduce claim on the temperature gradient between FZ and CD, i.e.

$$T_{\max_{FZ}} > T_{\max_{CD}} \quad (5)$$

Dependent on the specific energy (to reach a desired pulp quality), refining segment pattern as well as the refining segments condition due to wear, temperature difference in Eq.5 can vary within the interval 1-6 C. However, it is always important to get a gradient to facilitate peripheral steam evacuation.

To prevent large process variations due to e.g. disturbances in the chip feed rate to the flat zone (production), it is important to introduce controllers for the maximum temperatures in FZ and CD. This is indicated in Fig. 9 and Fig. 10, where the temperature responses vary considerably. This is also reflected in the distributed dynamic viscosity, see Fig. 10.

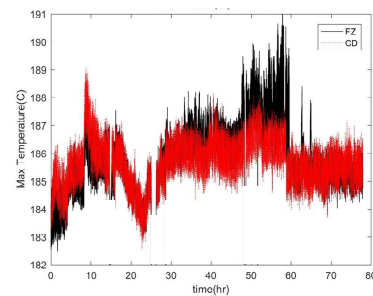


Fig. 9: Temperature maximum in FZ and CD, respectively.

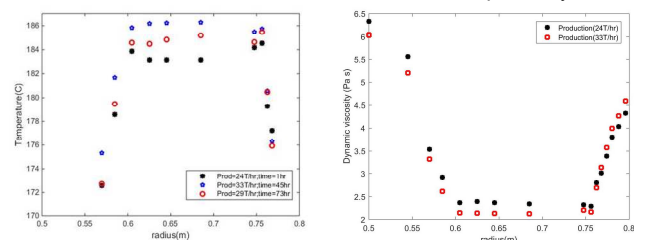


Fig. 10: Temperature profiles at the three production levels, 24, 29 and 33 T/hr and dynamic viscosity Pa\*s for the lowest and highest of the production levels in a CD82 refiner.

<sup>4</sup> The pulp quality can be described by at least three variables but normally only one of these is the prime candidate in control concepts.

Besides the information about the temperature profile changes at different process conditions, the use of the soft sensor for consistency profile estimation is vital to introduce in a control concept. In Fig. 11 the consistencies out from the refining zones are shown. During the test the motor load split in the refiner was changed dramatically, see Fig. 12, as the strategy was to distribute more work to the flat zone compared with the conical zone (at the same time as the consistencies in each zone were followed closely). This opened the possibility for an increased production rate.

It is interesting to see that the measured motor load in Fig. 8 is not affected so much when more work is applied to the flat zone, which also indicates that the split was not optimized before the test.

In short, the idea in the new control strategy for consistency control can also be illustrated by showing the ratios between the plate gaps, dilution water feed rates and consistencies in FZ and CD besides the maximum temperatures, see Fig. 13. When the production rate is increased it is obvious that the strategy is to keep a stable consistency ratio.

To verify the consistency estimation using the extended entropy model, manual tests were made in the blow-line out from the refiner, see Fig. 14. Note that, without the model, the internal variables in the flat zone are impossible to estimate. This is a huge step forward in the development of the second control strategies for CD refiners in general.

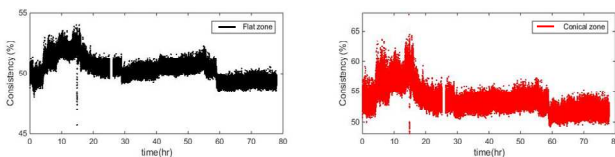


Fig. 11: Responses in the consistencies out from FZ and CD.

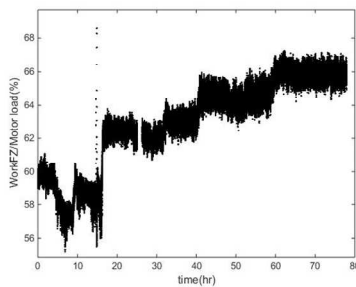


Fig. 12: Ratio between the estimated work in the flat zone and the total motor load.

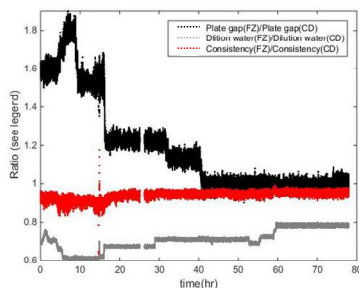


Fig. 13: The ratios between selected external and internal variables in the flat zone and conical zone. The ratios highlight the strategy to keep a stable consistency ratio when running the test according to Fig. 8.

Finally, as the motor load during the test was relatively stable, see Fig. 11, at the same time that the production could be increased from 24 to 33 ADMT/hr, the specific energy demand was ultimately reduced dramatically, by about 40%, see Fig. 15<sup>5</sup>. This also led to a situation where two small refiners could be closed down without violating the pulp and handsheet property specification.

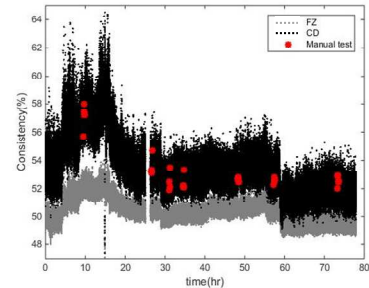


Fig. 14: Estimated consistencies out from the flat and conical zones together with manual consistency derived from samples in the blow-line.

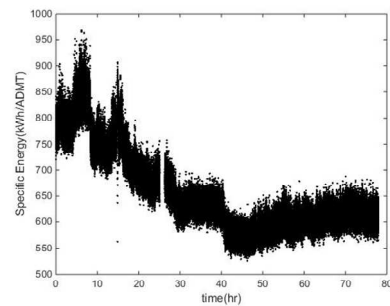


Fig. 15: Specific energy reduction when following the procedure outlined.

When increasing the production rate, it is always important to check the pulp specification in terms of the amount of shives in the sample. As seen in Fig. 16, both the long and wide measures for shives increase slightly. However, by tuning the consistency together with the temperature profile in the flat and conical zones, the increased shives can be reduced to normal levels. This was not performed during the test as the pulp specification was met.

However, future algorithms for pulp and handsheet property estimations, see Karlström and Hill (2016a,b,c) will be available to introduce as the last step to complement the control strategies I and II.

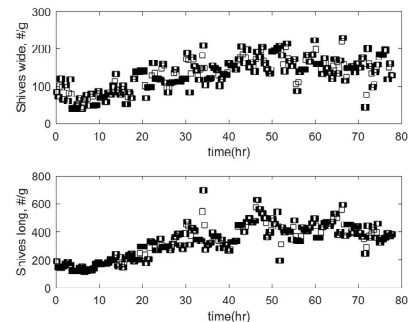


Fig. 16: Wide and long shives versus time.

<sup>5</sup> Similar results from a Jyhä SD65 refiner have been published earlier by Harkonen and Tienverri (1995).

**Example II:** Here, the topic is to estimate the consistency in the two zones of a Twin refiner. Knowing the steam and water mass flows based on the material and energy balances the entire consistency profile can be derived using the extended entropy model. However, the results are focused on the estimated outlet consistencies from each refining zone and the estimated weighted blow-line consistency which is verified using a measured blow-line consistency.

The reason why the consistency in each refining zone is important is that a variable consistency can affect the fiber residence time considerably, see Karlström and Hill (2014a). In Twin refiners, a consistency deviation between the FS and DS is thereby not a favourable situation. To overcome this, it is important to control the consistency individually on each side by manipulating the dilution water feed rate.

The consistency control loop, illustrated in Fig. 17 and Table 1, is based on a traditional cascade control concept for each refiner where the dilution water flow rate is controlled in the inner loop. It is obvious that this rudimentary control concept can be improved if the consistency in each refining zone can be controlled individually and this will be confirmed and validated in this paper.

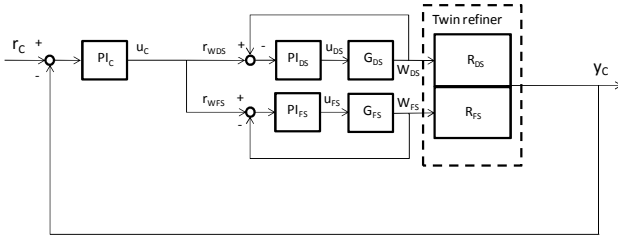


Fig. 17: Cascaded consistency control loop for a Twin refiner. The inner loop control the dilution water flow rate to the two refining zones that are called FS and DS, respectively.

Table 1: Description of notations used in Fig. 17.

	Description
$r_C$	Reference outer loop, consistency variable.
$y_C$	Output signal; the outer loop, measured consistency.
$W_{DS}, W_{FS}$	Dilution water to the refining zones ,DS and FS respectively.
$r_{WDS}, r_{WFS}$	Reference for the dilution water set points on DS and FS.
$u_C$	Dilution water change to adjust the control error. in the outer loop.
$u_{DS}, u_{FS}$	Dilution water change to adjust the control error, in the inner loop.
$PI_C$	Controller for the outer loop, consistency.
$PI_{DS}, PI_{FS}$	Controllers for the inner loop (Dilution water control).
$R_{DS}, R_{FS}$	The refining zones.

Suppose that the dilution water feed rates to FS and DS are changed in opposite directions according to the upper figure in Fig. 18.

During the first step changes in dilution water feed rates to FS and DS,  $t=\{0, 1.75\}hr$ , the valve opening is small in both directions which indicates that it is easy to feed water to both the FS and DS. At the same time, the plate gap is not affected at all, see Fig. 18.

During the period  $t=\{1.75, 2.25\}hr$ , when the dilution water feed rates are changed in opposite direction, the resistance to feed water to each zone is much higher on DS compared with FS. At the same time as the plate gap distance is changed considerably. This is most likely a

consequence of a shift in the steam balance in the refining zones.

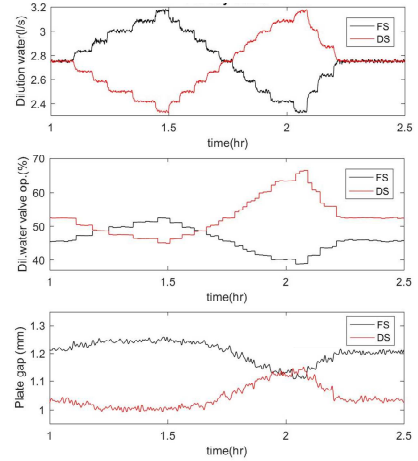


Fig. 18: Changes in dilution water feed rates and corresponding valve opening and plate gap changes.

The changes in plate gap are also reflected in the load conveyer effects, see Fig. 19.

To find the consistency in each refining zone we focus on the period between 1.75 and 2.25 hours. When estimating the consistencies using the extended entropy model, described in the main text, we get the responses in Fig. 20.

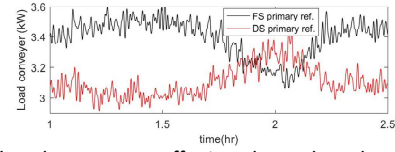


Fig. 19: Load conveyer effects when changing the dilution water feed rates according to Fig. 18.

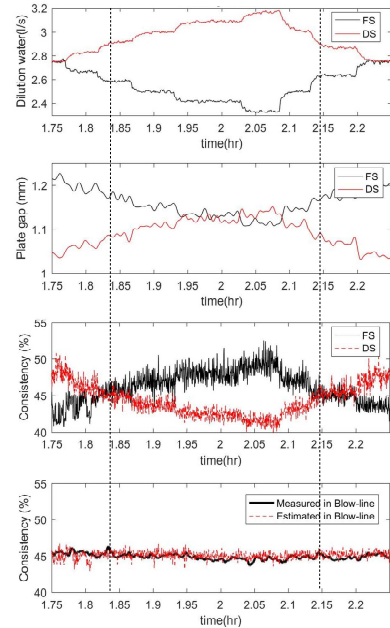


Fig. 20: Step changes in dilution water feed rates and the responses in the measured plate gaps and corresponding consistency estimates.

Unfortunately, these consistencies in FS and DS cannot be verified by measurements. However, by knowing the



weighted mass flows of pulp in each refining zone it is possible to estimate the consistency in the blow-line which can be validated by the measured consistency, see lower figure in Fig. 20.

Normally, when the plate gap is increased, the maximum temperature is reduced.

In this case, the temperature maximum on DS is increased when the plate gap is increased which indicates that more chips are fed to DS.

In those cases where the plate gap measurements are not available it is sometimes possible to use the effect ratio between the load conveyers (FS and DS respectively) instead of the plate gap ratio.

As seen in Fig. 21, the estimated consistency become almost identical and it is obvious that we have to do more tests before rejecting them as unimportant. However, this is not always true as we will see blow.

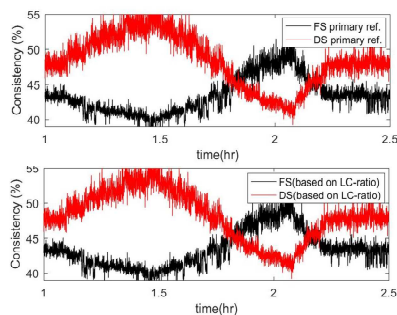


Fig. 21: Upper figure: Estimated consistency based on the plate gap ratio according to Eq. 1. Lower figure: Estimated consistency based on the load conveyer effect ratio.

To reproduce and validate the results, the dilution water feed rates were changed according to the upper figure in Fig. 22. The step changes results in valve openings according to the middle figure. The initial deviation between FS and DS in valve opening is negligible which means that the resistance to feed the refining zones are almost equal on FS and DS.

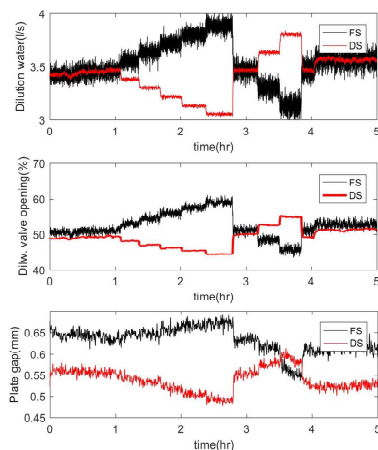


Fig. 22: Upper figure; Dilution water feed rate to the refining zones. Middle figure; Dilution water valve opening. Lower figure; Plate gaps. All in a primary Twin refiner<sup>6</sup>.

<sup>6</sup> The production was about 380.4 ADMT/day and the consistency control was not used in this test series.

It is interesting to compare the plate gap measurements in lower figure in Fig. 22, and the inlet temperature (closest to the breaker bars), see Fig. 23.

The inlet temperatures respond quite clear to the changes in the dilution water feed rate and moreover, it is more or less inversely proportional to the plate gap.

It is also interesting to see that the maximum temperatures, in the lower figure of Fig. 23, do not change much even though the plate gap change<sup>7</sup>.

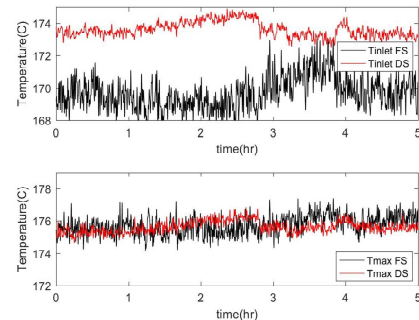


Fig. 23: Upper figure: Inlet temperature in each refining zone. Lower figure: Temperature maximum in each refining zone according to Fig. 22.

## Concluding remarks

The main purpose of this paper is to study how the internal variables (e.g. temperature, consistency, backward flowing steam and forces obtained when fibers interact with the refining bars) can be used in a new control concept. It is shown how they differ from the traditional external variables (e.g. dilution water feed rate, specific energy and plate clearance).

The consistency profile turns out to be invaluable when trying to optimize the refining process, develop new refining segment patterns etc. and they can be seen as the backbone of future control concepts of all types of refiners.

To keep track of the fiber development, it is important to stabilize the backward flowing steam. That is done in the work here by stabilizing the temperature profile. When the temperature profile is stabilized, both the fiber throughput and the consistency profile can be optimized to maintain the pulp quality variations within a pre-specified interval. This is illustrated in this paper by a test performed to maintain the ratio between the consistencies out from the flat and conical zones stable when increasing the production rate.

It is furthermore shown that the consistencies in the flat and conical zones in CD-refiners as well in FS and DS in Twin refiners are important internal variables that affect the pulp development when optimizing the process.

In summary, we can conclude that it is possible to optimize the process to meet a 40 % specific energy reduction without violating the pulp property

<sup>7</sup> For mills with no gap sensors installed the inlet temperature might be a good choice to use in primary refiners when searching for a more even consistency between the FS and DS.

specification in CD-refiners. Furthermore, practical work will of course also be performed in Twin refiners to further develop their energy efficiency potential. We believe that increased fundamental understanding of the role of distributed dynamic viscosity in refining in general is a key factor to find ways to further improve energy efficiency of refining.

---

## Acknowledgements

The authors gratefully acknowledge the funding of the Swedish Energy Agency, Andritz and Valmet, StoraEnso Skoghall and Hylte mills, for running trials and providing the excellent laboratory and process data used in this study. Special thanks to Jan Hill for all fruitful discussions.

---

## Literature

**Atack, D., & Stationwala, M. I. (1975).** On the measurement of temperature and pressure in the refining zone of an open discharge refiner. In *Technical Papers of the International Mechanical Pulping Conference*.

**Atack, D. (1981).** Dynamic mechanical loss properties of wood. *Philosophical Magazine A*, 43(3), 619-625.

**Berg, D. (2005):** A Comprehensive Approach to Modeling and Control of Thermomechanical Pulping Processes, Lic thesis. Dept. of Signals and Systems, Chalmers.

**Bird, R.B, Stewart W.R. and Lightfoot, E.N. (1960):** Transport phenomena, John Wiley and Sons Inc., New York.

**Björkqvist, T., Engberg, B. A., Salminen, L. I., & Salmi, A.**

(2012). Towards optimal defibration: Energy reduction by fatiguing pre-treatment. *Nordic Pulp & Paper Research Journal*, 27(2), 168-172.

**Dahlqvist G. and Ferrari B. (1981)** Mill operating experience with a TMP refiner control system based on a true disc clearance measurement, Int. Mech. Pulping Conf., Oslo, Norway, Session III, no. 6.

**Engstrand, P., Ottestam, C., Salmen, L., Pettersson, R., Sjögren, B., & Htun, M. (1991).** The relationship between ionizable groups and swelling potential of wood fibers. *STFI-Meddelande. Serie A (Sweden)*.

**Engstrand, P. (2011).** Filling the gap – improved energy efficiency and quality stability in mechanical pulp refining. In *International Mechanical Pulping Conference 2011, Xian China* (pp. 546-549). China Light Industry Press.

**Engstrand, P. O., Engberg, B. A., & Eriksson, K. (Eds.). (2014).** Filling the Gap: Final Report. Mittuniversitetet.

**Eriksson, K. (2005):** An Entropy-based Modeling Approach to Internally Interconnected TMP Refining Processes, Licentiate thesis, Chalmers University of Technology, Göteborg, Sweden. University of Technology, ISSN 1403-266x; nr R034/2005.

**Eriksson, K. (2009):** Towards improved control of TMP refining processes, PhD thesis, Chalmers University of Technology, Göteborg, Sweden.

**Fjellström, H., Engstrand, P., & Htun, M. (2012).** Aspects of fibre wall swelling in high-yield pulp. In *4th International Conference on Pulping, Papermaking and Biotechnology (ICCPB'12), Nanjing, China, Nov 7–9* (pp. 1183-1186).

**Fjellström, H., Engstrand, P., & Htun, M. (2013).** On the relationship between wood fibre wall swelling, charged groups, and delamination during refining. In *J-FOR-JOURNAL OF SCIENCE & TECHNOLOGY FOR FOREST PRODUCTS AND PROCESSES* (Vol. 3, No. 4, pp. 30-34).

**Harkonen, E., Tienveri, T. (1995):** The influence of production rate on refining in a specific refiner. *Int. Mech. Pulp. Conf.* Ottawa, Canada p. 177.

**Hill, J., Westin, H., and Bergstrom, R. (1979)** Monitoring pulp quality for process control, *Int. Mech. Pulping Conf.*, Toronto, Canada, p. 111-125.

**Hill, J., Saarinen, K., Stenros, R. (1993)** On the control of chip refining systems, *Pulp and Paper Canada*, 94(6), p. 43-47.

**Holmgren, S. E., Svensson, B. A., Gradin, P. A., & Lundberg, B. (2008).** An encapsulated split Hopkinson pressure bar for testing of wood at elevated strain rate, temperature, and pressure. *Experimental Techniques*, 32(5), 44-50.

**Honkasalo, J.V., Polkkynen, E.E., Vainio, J.A., (1989)** Development of control systems in mechanical pulping (GW, TMP) at Rauma, *Int. Mech. Pulping Conf.*, Helsinki, Finland, p. 376-389

**Johansson B.-L., Karlsson H., Jung, E., (1980)** Experiences with computer control, based on optical sensors for pulp quality, of a two-stage TMP-plant, 1980 Process Control Conf., Halifax, Nova Scotia, p. 145-152.

**Karlström, A., Berg, D. and Eriksson, K. (2005):** Developments in soft sensors for measurement of refining parameters, Scientific and technical advances in refining and mechanical pulping, Barcelona, Spain, 28 Feb.-4 Mar. 2005, Pira International, Leatherhead, UK, Paper 5.

**Karlström, A., Eriksson, K., Sikter, D. and Gustavsson, M. (2008):** Refining models for control purposes, *Nord. Pulp Paper Res. J* 23(1), 129.

**Karlström, A., and Isaksson, A. (2009):** Multi-rate optimal control of TMP refining processes, *Int. Mech. Pulping Conf.*, Sundsvall, Sweden.

**Karlström, A., (2013):** Multi-scale modeling in TMP-processes, 8<sup>th</sup> Int. Fundamental Mech. Pulp Res. Seminar, Åre, Sweden.

**Karlström, A. and Eriksson, K. (2014a):** Refining energy efficiency Part I: Extended entropy model. *Nord. Pulp Paper Res. J.* 29(2).

**Karlström, A. and Eriksson, K. (2014b):** Refining energy efficiency Part II: Forces acting on the refining bars. *Nord. Pulp Paper Res. J.* 29(2).

**Karlström, A. and Eriksson, K. (2014c):** Refining energy efficiency Part III: Modeling of fiber-to-bar interaction. *Nord. Pulp Paper Res. J.* 29(3)

**Karlström, A. and Eriksson, K. (2014d):** Refining energy efficiency Part IV: Multi-scale modeling of refining processes. *Nord. Pulp Paper Res. J.* 29(3).

**Karlström, A. and Hill J. (2014a):** Refiner Optimization and Control Part I: Fiber residence time and major dynamic fluctuations in TMP refining processes. *Nord. Pulp Paper Res. J.* 29(4).

**Karlström, A. and Hill J. (2014b):** Refiner Optimization and Control Part II: Test procedures for describing dynamics in TMP refining processes. *Nord. Pulp Paper Res. J.* 29(4)

**Karlström, A. and Hill J. (2015a):** Refiner Optimization and Control Part III: Natural decoupling in TMP refining processes. *Nord. Pulp Paper Res. J.* 30(3).

**Karlström, A., Eriksson, K. and Hill J. (2015b):** Refiner Optimization and Control Part IV: Long term follow up of control performance in TMP processes. *Nord. Pulp Paper Res. J.* 30(3).

**Karlström, A., Hill J., Ferritsius, R. and Ferritsius, O.** (2015): Pulp Property Development Part I: Interlacing Undersampled Pulp Properties and TMP Process Data using Piece-wise Linear Functions. *Nord. Pulp Paper Res. J.* 30(4), 599-608.

**Karlström, A., Hill J., Ferritsius, R. and Ferritsius, O.** (2016a): Pulp Property Development Part II: Process Nonlinearities and its Influence on Pulp Property Development. Submitted for publication in *Nord. Pulp Paper Res. J.*

**Karlström, A., Hill J., Ferritsius, R. and Ferritsius, O.** (2016b): Pulp Property Development Part III: Fiber Residence Time and Consistency Profile Impact on Specific Energy and Pulp Properties. Submitted for publication in *Nord. Pulp Paper Res. J.*

**Kure, K.-A** (1999): On the relationship between process input variables and fiber characteristics in thermomechanical pulping, PhD thesis 45:99, Norwegian Univ. Science and Technology, Trondheim.

**Lehtonen, S., Virtanen, P., Lindeberg, M., Fralic, G. A.,** (2014): New TMP optimization approach: using advanced quality control to stabilize tensile strength and reduce power cost. International Mechanical Pulping Conference, Helsinki, Finland.

**Engberg, B., Logenius, L., & Engstrand, P.** (2014). Mechanical properties of sulphonated wood in relation to wing refiner properties. In *International Mechanical Pulping Conference, IMPC 2014; Helsinki; Finland; 2 June 2014 through 5 June 2014; Code 109275*. Paper Engineers' Association (PI).

**Miles, K. B. and May, W. D.** (1990): The Flow of Pulp in Chip Refiners, *J. Pulp Paper Sci.* 16(2), 63.

**Miles, K. B. and May, W. D.** (1991): Predicting the performance of a chip refiner: A constitutive approach, *Int. Mech. Pulping Conf.* p 295-301.

**Moilanen, C. S., Björkqvist, T., Engberg, B. A., Salminen, L. I., & Saarenrinne, P.** (2016). High strain rate radial compression of Norway spruce earlywood and latewood. *Cellulose*, 23(1), 873-889.

**Murton, K., Duffy, G., Corson, S.** (2002): Pulp residence time influence on refining intensity and pulp quality, *Proceedings of 56<sup>th</sup> Appita Annual Conference*, Carlton, pp. 185-193.

**Oksum J.,** (1983) New technology in the Skogn mechanical pulp mill, *Int. Mech. Pulping Conf.*, Washington DC, USA, p. 143-153.

**Sabourin, M., Wiseman, N. and Vaughn, J.** (2001): Refining theory considerations for assessing pulp properties in the commercial manufacture of TMP. *55<sup>th</sup> Appita Annual Conference*, p 195-204.

**Salmi, A., Salminen, L. I., Engberg, B. A., Björkqvist, T., & Hæggström, E.** (2012). Repetitive impact loading causes local plastic deformation in wood. *Journal of Applied Physics*, 111(2), 024901.

**Stationwala, M. T., Attack, D., Wood, J. R., Wild, D. J., & Karnis, A.** (1991). The effect of control variables on refining zone conditions and pulp properties. *Paperi ja puu*, 73(1), 62-69.

**Strand, B.C., Mokvist, A., Falk, B., Jackson, M.** (1993): The effect on production rate on specific energy consumption in high consistency chip refining, *IMPC 1993*, pp. 143.

**Strand, B.C.** (1996): Model based control of high consistency refining, *TAPPI Journal* 79(10), pp.140-146.

**Strand, B.C., Grace, B.** (2014): Implementation of advanced supervisory control within a TMP refiner quality control system, *International Mechanical Pulping Conference*, Helsinki, Finland.

**Svensson, B. A., Rundlöf, M., & Höglund, H.** (2006). Sliding friction between wood and steel in a saturated steam environment. *Journal of pulp and paper science*, 32(1), 38-43.

## Appendix

In short, the entropy generation can be expressed as

$$dS(r) = m_i c_p \ln\left(\frac{T(r+dr)}{T(r)}\right) + \sum_{j=2}^3 (m_j(r+dr)s_j(r+dr) - m_j(r)s_j(r))$$

$$w_{th}(r) 2\pi r dr = m_i c_p (T(r+dr) - T(r)) + \sum_{j=2}^3 (m_j(r+dr)h_j(r+dr) - m_j(r)h_j(r))$$

which gives

$$\frac{w_R(r)}{T(r)} 2\pi r dr = m_i c_p \ln\left(\frac{T(r+dr)}{T(r)}\right) + \sum_{j=2}^3 (m_j(r+dr)s_j(r+dr) - m_j(r)s_j(r))$$

$$m_2(r) + m_3(r) = m_2(r+dr) + m_3(r+dr)$$

$w_R \neq 0$  and  $q_{loss} \approx 0$

$m_1^{in} = m_1^{out} = m_1$ ,  $m_2^{in}$  and  $m_3^{in}$  are known  $\Rightarrow$

$m_2^{in} + m_3^{in} = m_2^{out} + m_3^{out} \Rightarrow m_2^{out} = m_2^{in} + m_3^{in} - m_3^{out}$

$dr = r_{out} - r_{in}$

Find  $m_3^{out}$ ,  $w_{th}$  and  $w_{def}$

$$X = \frac{w_{R_{in}}}{T_{in}} 2\pi r_{in} dr - m_i c_p \ln\left(\frac{T_{out}}{T_{in}}\right) - m_2^{in}(s_2^{out} - s_2^{in}) - m_3^{in}(s_2^{out} - s_3^{in})$$

$$Y = m_i c_p (T_{out} - T_{in}) + m_2^{out} h_2^{out} - m_2^{in} h_2^{in} + m_3^{out} h_3^{out} - m_3^{in} h_3^{in}$$

$$m_3^{out} = X / (s_3^{out} - s_2^{out})$$

$$w_{th_{in}} = Y / (2\pi r dr)$$

$$w_{def_{in}} = w_{R_{in}} - w_{th_{in}}$$

Table 1: Latin symbols

Symbol	Description
$c_p$	Heat capacity
$dS$	Entropy generation
$h_i$	Specific enthalpy of component $i$
$m_i$	Material of component $i$
$q_{loss}$	Energy losses per unit area
$r$	Radial coordinate
$s_i$	Specific entropy of component $i$
$S$	Total entropy
$T$	Temperature
$w_{th}$	Thermodynamic work per unit area
$w_{def}$	Refining work per unit area
$w_R$	Estimated total work per unit area

Table 2: Greek symbols

Symbol	Description
$\delta$	Viscous dissipation
$\mu$	Dynamic viscosity
$\omega$	Angular speed of the refiner disc
$\Delta$	Plate gap at radius $r$

Table 3: Indices

Sub-&Superscript	Description
$1$	Wood/Pulp phase
$2$	Water phase
$3$	Steam phase
$in$	Refiner inlet
$out$	Refiner outlet

As seen above, this gives the defibration work,  $w_{def}$ , and thermodynamical work,  $w_{th}$ , in the refining zone, and it is the knowledge of the mass flows of pulp ( $m_1$ ) and water ( $m_2$ ) as a function of the radius that provides the possibility to derive the consistency profile in the refining zone as

$$C(r) = m_1 / (m_1 + m_2)$$

To fully understand the modeling efforts when deriving soft sensors, it is important to model geometrical properties as well. Even though such properties, in terms of refining segment patterns, directly affect the shape of the temperature profile, the position of the contraction of the refining segments plays a vital role from a geometrical perspective.

Moreover, this position indicates how much the shear force will change under certain conditions, and Karlström and Eriksson (2014a,b) showed that this was not well described. They showed that the plate gap,  $\Delta_{gap}$ , which is measured in one radial position along the radius, is not sufficient as an input and that information is needed about the radially dependent distance between the refining segments,  $\Delta(r)$ , which also include the taper  $\Delta_{taper}(r)$ , see Fig. 25.

Hence, according to Fig. 25, the distance between the refining surfaces can be expressed as

$$\Delta(r) = 2\Delta_{taper}(r) + \Delta_{gap}$$

As indicated above, the geometrical perspective in terms of the segment pattern must also be considered in the model as it clearly influences the refining conditions and thereby the process performance. The effective cross sectional surface, see Fig. 26, must therefore be included when deriving physical variables in the refining zone.

There is a large variety in segment design parameters, and variations in patterns along the radius must be considered in the model as they affect e.g. the pulp residence time as well as the fiber development itself. The bar density is set to

$$\eta(r) = B(r) / (B(r) + G(r))$$

where  $B(r)$  and  $G(r)$  are vectors and define the bar and groove width along the radius of the refining segments. It is obvious that the bar density must be considered when describing the cross-sectional area that is available for the fibers on their path from any position along the radius to the periphery of the segments.

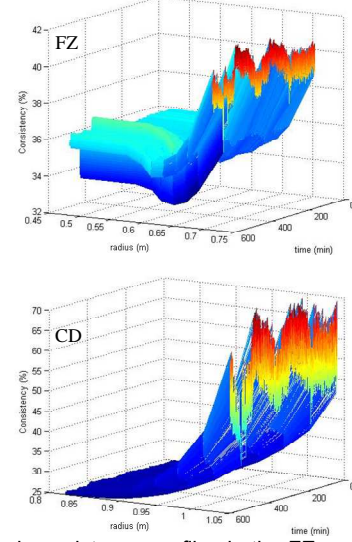


Fig. 24: Typical consistency profiles in the FZ and CD zones as functions of radial position and time.

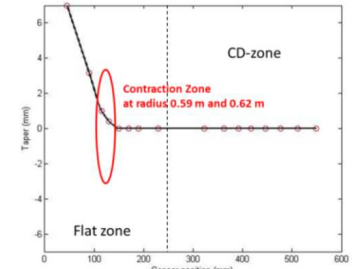


Fig. 25: The taper,  $\Delta_{taper}(r)$ , describing one side of the segments in the flat zone and CD zone, respectively. Note that the plate gaps,  $\Delta_{gap}$ , in the flat zone and the CD zone are not included in this figure.

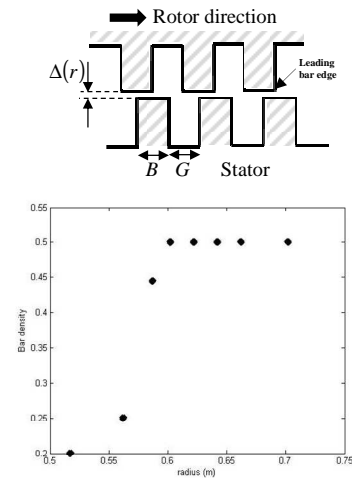


Fig. 26: Upper: Cross section of a hypothetical refiner segment. Lower: Bar density for typical segments in a CD refiner.



In the literature, the fiber residence time  $\tau$  is exclusively related to the pulp without considering the effect of chip, pulp, and fiber interaction with steam and free water (at the beginning of the refining zone). Karlström and Eriksson (2014a,b) commented on this point, but the theory was only vaguely linked to the residence time via the chip, pulp and fiber viscosity variations. To simplify the description, we prefer to describe the residence time as the fiber residence time, i.e. the average transport time of fibers from the inner part of the refining zone to the outside rim of the refining segments

$$\tau = \int_{r_{in}}^{r_{out}} \frac{1}{v_1(r)} dr = \int_{r_{in}}^{r_{out}} \frac{\rho_1(r) A_1}{m_1(r)} dr$$

The density,  $\rho_1$ , mass flow,  $m_1$ , cross-area available for the pulp,  $A_1$ , and residence time,  $\tau$ , between arbitrary positions in the refining zone  $\{r_{in}, r_{out}\}$  can therefore be estimated as well. The volumetric flows must be considered to find the cross-area available for the pulp,  $A_1$ . The steam flow,  $V_3$ , is much larger than the volumetric flows of pulp  $V_1$  and water  $V_2$  together, i.e.  $abs(V_3) \gg (V_1 + V_2)$ . In the extended entropy model it is shown that the vapor velocity,  $v_3$ , is much larger than the pulp velocity,  $v_1$ , in the refiner, see Karlström and Hill (2014a). As a result, the vapor is assumed to diffuse faster into the grooves as compared with the pulp due to the tangential pressure drop and the radial pressure drop. The interplay between the tangential and radial pressure gradients is complex, but it is important to stress when discussing intricate fluid dynamics between the refining segments; here it is assumed that the volumetric steam flow is primarily localized at the grooves. The major part of the moving pulp, including the bounded water, will thereby be localized to the cross-sectional area between the bars and a hypothetical boundary layer between the stator and the rotor where the steam flow is not dominant.

From the assumption  $v_1(r) = v_2(r)$ , the cross-sectional area for the water will be  $A_2 = A_1 V_2 / V_1$ . Knowing the refining segment geometry, we also know the total cross-sectional area,  $A_{TOT}$ . The total volumetric flow,  $V_{TOT}$ , is known from the extended entropy model, see the discussion above. Together with the derived vapor velocity, which is much larger than the pulp velocity, i.e.  $v_3(r) \gg v_1(r)$ , the cross-sectional area for the vapor can be derived.

$$A_1 = \frac{V_1}{V_1 + V_2} (A_{TOT} - A_3)$$

$$A_3 \ll \frac{V_3}{V_1} A_1 = \frac{V_3}{V_1 + V_2} (A_{TOT} - A_3) \Rightarrow A_3 \left( \frac{V_{tot}}{V_1 + V_2} \right) \ll \frac{V_3}{V_1 + V_2} A_{TOT}$$

$$A_3 \ll \frac{V_3}{V_{TOT}} A_{TOT}$$

However,  $V_3 \approx V_{TOT}$ , which means that  $A_3 \ll A_{TOT}$ , i.e.

$$\begin{cases} A_{fz} \approx \frac{V_{fz}}{V_{fz} + V_{2fz}} A_{TOTfz} \\ A_{cd} \approx \frac{V_{cd}}{V_{cd} + V_{2cd}} A_{TOTcd} \end{cases}$$